MOLECULAR AND ATOMIC SPECTROSCOPY



Thomas Wenzel
Bates College

LibreTexts™

TABLE OF CONTENTS

00: Front Matter

Table of Contents

1.1: General Background on Molecular Spectroscopy

1.2: Ultraviolet/Visible Absorption Spectroscopy

1.3: Molecular Luminescence

1.4: Infrared Spectroscopy

1.5: Raman Spectroscopy

1.6: Atomic Spectroscopy

1.7: Supplemental NMR Topics

This page titled Molecular and Atomic Spectroscopy (Wenzel) is shared under a CC BY-NC 4.0 license and was authored, remixed, and/or curated by Thomas Wenzel via source content that was edited to the style and standards of the LibreTexts platform.

- Molecular and Atomic Spectroscopy (Wenzel) by Thomas Wenzel is licensed CC BY-NC 4.0. Original source: http://community.asdlib.org/activelearningmaterials/molecular-and-atomic-spectroscopy/.

1.1: General Background on Molecular Spectroscopy

Learning Objectives

After completing this unit the student will be able to:

- Explain what it means to use spectroscopic methods for qualitative and quantitative analysis.
- Identify the terms in and describe deviations to Beer's Law.
- Describe the effect of changing the slit width and the impact it will have on qualitative and quantitative analyses.
- Qualitatively determine the relative error in absorbance measurements and determine the optimal range for measurement purposes.
- Describe the desirable features of a radiation source. 6. Explain the advantages of a dual versus single-beam spectrophotometer.
- Explain the difference between a 3- and 4-level laser and why it is not possible to have a 2-level laser.
- Compare the output of and advantages of prisms and gratings as dispersing elements.
- Explain how a photomultiplier tube works.
- Explain how an array detector works and describe the advantages of using an array detector.

This page titled 1.1: General Background on Molecular Spectroscopy is shared under a CC BY-NC 4.0 license and was authored, remixed, and/or curated by Thomas Wenzel via source content that was edited to the style and standards of the LibreTexts platform.

- 1: General Background on Molecular Spectroscopy by Thomas Wenzel is licensed CC BY-NC 4.0. Original source: https://asdlib.org/activelearningmaterials/molecular-and-atomic-spectroscopy.

1.2: Ultraviolet/Visible Absorption Spectroscopy

Learning Objectives

After completing this unit the student will be able to:

- Compare and contrast atomic and molecular spectra.
- Explain why atomic spectra consist of lines whereas molecular spectra at room temperature are broad and continuous.
- Justify the difference in molecular spectra at room temperature and 10 K.
- Describe the cause of Doppler broadening.
- Determine the effect of conjugation on a UV/Vis absorption spectrum.
- Determine the effect of non-bonding electrons on a UV/Vis absorption spectrum.
- Determine the effect of solvent on the energy of $n - pi^*$ and $\pi - \pi^*$ transitions.
- Evaluate the utility of UV/Vis spectroscopy as a qualitative and quantitative method.
- Describe a procedure by which UV/Vis spectroscopy can be used to determine the pKa of a weak acid.

Template:HideTOC

This page titled 1.2: Ultraviolet/Visible Absorption Spectroscopy is shared under a CC BY-NC 4.0 license and was authored, remixed, and/or curated by Thomas Wenzel via source content that was edited to the style and standards of the LibreTexts platform.

- 2: Ultraviolet/Visible Absorption Spectroscopy by Thomas Wenzel is licensed CC BY-NC 4.0. Original source: https://asdlib.org/activelearningmaterials/molecular-and-atomic-spectroscopy.

1.3: Molecular Luminescence

Learning Objectives

After completing this unit the student will be able to:

- Describe the difference between a singlet and triplet state.
- Draw an energy level diagram and identify the transitions that correspond to absorption, fluorescence, internal conversion, radiationless decay, intersystem crossing and phosphorescence.
- Explain why phosphorescence emission is weak in most substances.
- Draw a diagram that shows the layout of the components of a fluorescence spectrophotometer.
- Describe the difference between a fluorescence excitation and emission spectrum.
- Draw representative examples of fluorescence excitation and emission spectra.
- Describe a procedure for measuring phosphorescence free of any interference from fluorescence.
- Justify why fluorescence measurements are often more sensitive than absorption measurements.
- Describe the meaning and consequences of self-absorption.
- Identify variables including the effect of pH that can influence the intensity of fluorescence.
- Identify the features that occur in organic molecules that are likely to have high fluorescent quantum yields.
- Compare two molecules and determine which one will undergo more collisional deactivation.

Luminescent methods refer to a family of techniques in which excited state species emit electromagnetic radiation. Among luminescent methods are various sub-categories that include the processes of fluorescence, phosphorescence, chemiluminescence, bioluminescence and triboluminescence. Among these different sub-categories, fluorescence spectroscopy is by far the most common technique used for analysis purposes. You are no doubt familiar with fluorescent lights. This unit will allow you to understand how such a light works.

Template:HideTOC

This page titled 1.3: Molecular Luminescence is shared under a CC BY-NC 4.0 license and was authored, remixed, and/or curated by Thomas Wenzel via source content that was edited to the style and standards of the LibreTexts platform.

- 3: Molecular Luminescence by Thomas Wenzel is licensed CC BY-NC 4.0. Original source: https://asdlib.org/activelearningmaterials/molecular-and-atomic-spectroscopy.

1.4: Infrared Spectroscopy

Learning Objectives

After completing this unit the student will be able to:

- Describe the selection rule for infrared-active transitions.
- Determine the vibrations for a triatomic molecule and identify whether they are infrared-active.
- Draw the design of a non-dispersive infrared spectrophotometer and describe how it functions.
- Describe the difference between time and frequency domain spectra.
- Explain how a Michelson Interferometer can be used to obtain a time domain spectrum.
- Explain the advantages of Fourier Transform infrared spectroscopy over conventional infrared spectroscopy.

This page titled 1.4: Infrared Spectroscopy is shared under a CC BY-NC 4.0 license and was authored, remixed, and/or curated by Thomas Wenzel via source content that was edited to the style and standards of the LibreTexts platform.

- 4: Infrared Spectroscopy by Thomas Wenzel is licensed CC BY-NC 4.0. Original source: https://asdlib.org/activelearningmaterials/molecular-and-atomic-spectroscopy.

1.5: Raman Spectroscopy

Learning Objectives

After completing this unit the student will be able to:

- Determine whether the molecular vibrations of a triatomic molecule are Raman active.
- Explain the difference between Stokes and anti-Stokes lines in a Raman spectrum.
- Justify the difference in intensity between Stokes and anti-Stokes lines.
- Draw the Stokes and anti-Stokes lines in a Raman spectrum of a compound when given the energies of the different transitions.

Raman spectroscopy is an alternative way to get information about the infrared transitions within a molecule. In order for a vibrational transition to be Raman active, the molecule must undergo a change in polarizability during the vibration. Polarizability refers to the ease of distorting electrons from their original position. The polarizability of a molecule decreases with increasing electron density, increasing bond strength, and decreasing bond length.

Consider the molecular vibrations of carbon dioxide and determine whether or not they are Raman active.

The symmetric stretch of carbon dioxide is not IR active because there is no change in the net molecular dipole (Figure 1.5.1). Since both bonds are stretched (i.e., lengthened), both bonds are more easily polarizable. The overall molecular polarizability changes and the symmetric stretch is Raman active.

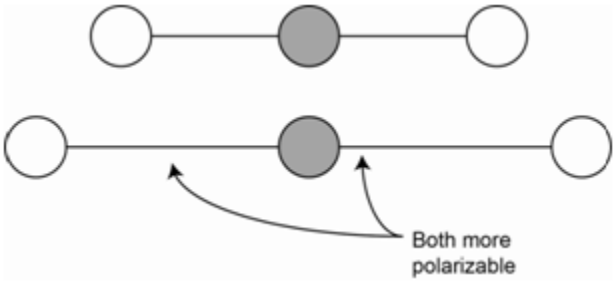


Figure 1.5.1: Representation of the Raman active symmetric stretch of carbon dioxide.

The asymmetric stretch of carbon dioxide is IR active because there is a change in the net molecular dipole (Figure 1.5.2). In the asymmetric stretch, one bond is stretched and is now more polarizable while the other bond is compressed and is less polarizable. The change in polarizability of the longer bond is exactly offset by the change in the shorter bond such that the overall polarizability of the molecule does not change. Therefore, the asymmetric stretch is not Raman active.

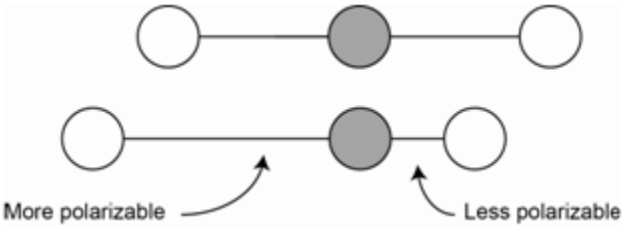


Figure 1.5.2: Representation of the Raman inactive asymmetric stretch of carbon dioxide.

The bending motion of carbon dioxide is IR active because there is a change in the net molecular dipole (Figure 1.5.3). Since the bending motion involves no changes in bond length, there is no change in the polarizability of the molecule. Therefore, the bending motion is not Raman active.

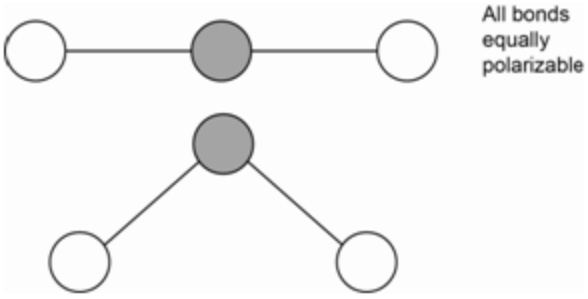


Figure 1.5.3: Representation of the Raman inactive bending vibration of carbon dioxide.

Note that the IR active vibrations of carbon dioxide (asymmetric stretch, bend) are Raman inactive and the IR inactive vibration (symmetric stretch) is Raman active. This does not occur with all molecules, but often times, the IR and Raman spectra provide complementary information about many of the vibrations of molecular species. Raman spectra are usually less complex than IR spectra.

An intriguing aspect of Raman spectroscopy is that information about the vibrational transitions is obtained using visible radiation. The process involves shining monochromatic visible radiation on the sample. The visible radiation interacts with the molecule and creates something that is known as a **virtual state**. From this virtual state it is possible to have a modulated scatter known as Raman scatter. Raman scatter occurs when there is a momentary distortion of the electrons in a bond of a molecule. The momentary distortion means that the molecule has an induced dipole and is temporarily polarized. As the bond returns to its normal state, the radiation is reemitted as Raman scatter.

One form of the modulated scatter produces **Stokes lines**. The other produces **anti-Stokes lines**. Stokes lines are scattered photons that are reduced in energy relative to the incident photons that interacted with the molecule. The reductions in energy of the scatter photons are proportional to the energies of the vibrational levels of the molecule. Anti-Stokes lines are scattered photons that are increased in energy relative to the incident photons that interacted with the molecule. The increases in energy of the scatter photons are proportional to the energies of the vibrational levels of the molecule.

The energy level diagram in Figure 1.5.4 shows representations for IR absorption, Rayleigh scatter, Stokes Raman scatter and anti-Stokes Raman scatter. For Stokes lines, the incident photons interact with a ground state molecule and form a virtual state. The scattered photons come from molecules that end up in excited vibrational states of the ground state, thereby explaining why they are lower in energy than the incident photons. For anti-Stokes lines, the incident photons interact with a molecule that is vibrationally excited. The virtual state produced by this interaction has more energy than the virtual state produced when the incident photon interacted with a ground state molecule. The scattered photons come from molecules that end up in the ground state, thereby explaining why they are higher in energy than the incident photons.

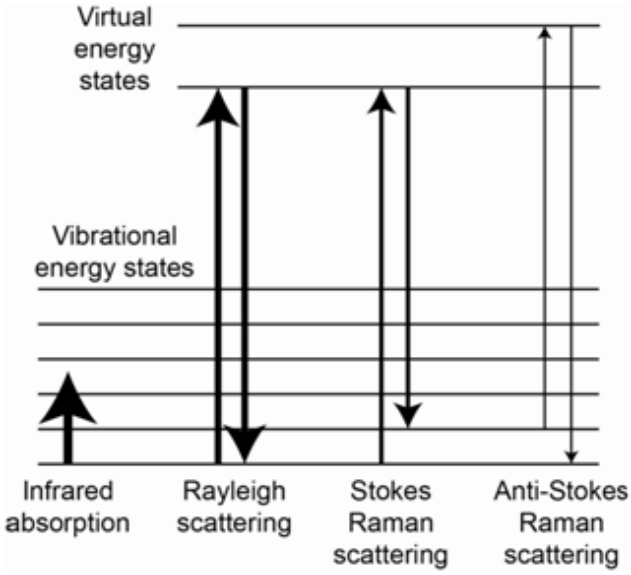


Figure 1.5.4: Energy level diagram showing the origin or infrared absorption, Rayleigh scatter, Stokes Raman scatter, and anti-Stokes Raman scatter.

It is important to recognize that, while the processes in Figure 1.5.4 responsible for Raman scatter might look similar to the process of fluorescence, the process in Raman spectroscopy involves a modulated scatter that is different from fluorescence. How do we know this? One reason is that Raman scatter occurs when the incident radiation has energy well away from any absorption band of the molecule. Therefore, the molecule is not excited to some higher electronic state but instead exists in a virtual state that corresponds to a high energy vibrational state of the ground state. Another is that Raman scatter has a lifetime of 10^{-14} second, which is much faster than fluorescent emission.

Which set of lines, Stokes or anti-Stokes, is weaker?

The anti-Stokes lines will be much weaker than the Stokes lines because there are many more molecules in the ground state than in excited vibrational states.

What effect would raising the temperature have on the intensity of Stokes and anti-Stokes lines?

Raising the temperature would decrease the population of the ground state and increase the population of higher energy vibrational states. Therefore, with increased temperature, the intensity of the Stokes lines would decrease and the intensity of the anti-Stokes lines would increase. However, the Stokes lines would still have higher intensity than the anti-Stokes lines.

Because scatter occurs in all directions, the scattered photons are measured at 90^{o} to the incident radiation. Also, Raman scatter is generally a rather unfavorable process resulting in a weak signal.

What would be the ideal source to use for measuring Raman spectra?

The more incident photons sent in to the sample, the more chance there is to produce molecules in the proper virtual state to produce Raman scattering. Since the signal is measured over no background, this suggests that we want a high power source. That means that a laser would be preferable as a source for measuring Raman spectra. The highly monochromatic emission from a laser also means that we can more accurately measure the frequency of the Stokes lines in the resulting spectrum. Also an array detector is preferable as it enables the simultaneous measurement of all of the scattered radiation.

The molecule carbon tetrachloride (CCl_4) has three Raman-active absorptions that occur at 218, 314 and 459 cm^{-1} away from the laser line. Draw a representation of the Raman spectrum of CCl_4 that includes both the Stokes and anti-Stokes lines.

The spectrum in Figure 1.5.5 shows a representation of the complete Raman spectrum for carbon tetrachloride and includes the Stokes and anti-Stokes lines. The laser line undergoes an elastic scattering known as Rayleigh scatter and a complete spectrum has a peak at the laser line that is far more intense than the Raman scatter. Note that the anti-Stokes lines are lower in intensity and higher in energy than the Stokes lines. Note as well that the two spectra appear as mirror images of each other with regards to the placement of the bands at 218, 314 and 459 cm^{-1} away from the Rayleigh scatter peak.

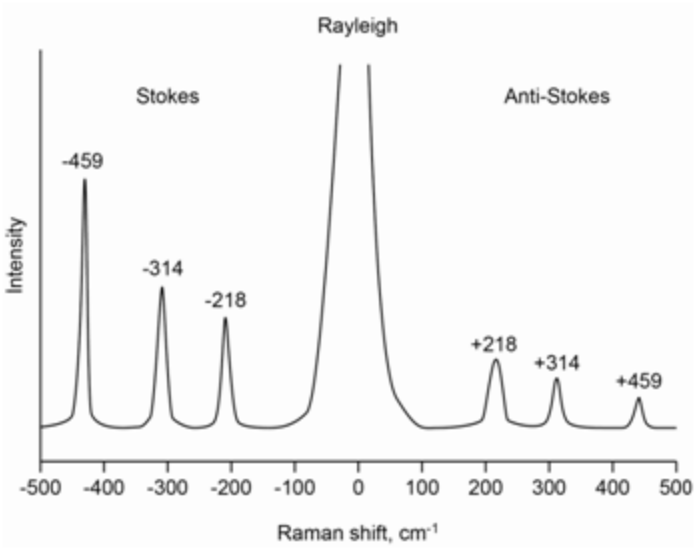


Figure 1.5.5: Complete Raman spectrum of carbon tetrachloride (CCl_4).

The energy level diagram in Figure 1.5.6 shows the origin of all of the lines and inspection of it should rationalize why the placement of the Stokes and anti-Stokes lines are mirror images of each other. The relative intensity of the three Stokes lines depends on the probability of each scatter process and is something we could not readily predict ahead of time.

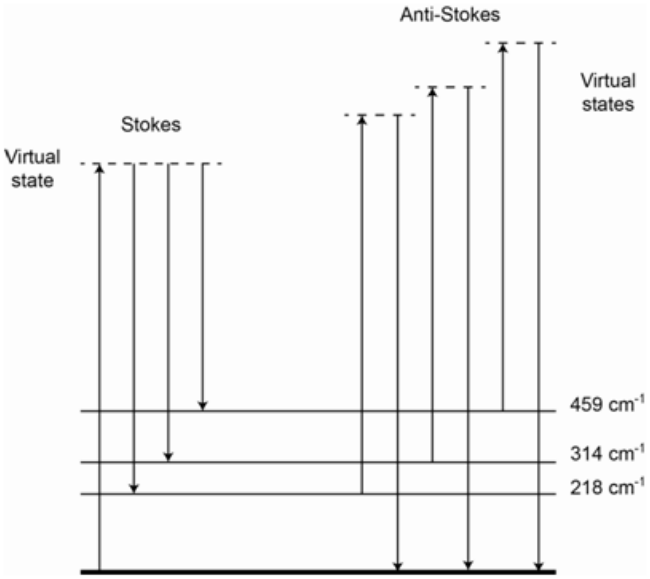


Figure 1.5.6: Energy level diagram showing the origin of Stokes and anti-Stokes lines in the Raman spectrum of carbon tetrachloride (CCl_4).

Why do the anti-Stokes lines of carbon tetrachloride have the following order of intensity: 219 > 314 > 459 cm^{-1}?

The intensity of the three anti-Stokes lines drops going from the 218 to 314 to 459 cm^{-1} band. Anti-Stokes scatter requires an interaction of the incident photon with vibrationally excited molecules. Heat in the system causes some molecules to be vibrationally excited. The drop in intensity is predictable because, as the vibrational levels increase in energy, they would have lower populations and therefore fewer molecules to produce Raman scatter at that transition.

Raman spectroscopy is an important tool used in the characterization of many compounds. As we have already seen, because the selection rules for Raman (change in polarizability) are different than infrared (change in the dipole moment) spectroscopy, there are some vibrations that are active in one technique but not the other. Water is a weak Raman scatterer and, unlike infrared

spectroscopy, where water has strong absorptions, water can be used as a solvent. Glass cells can be used with the visible laser radiation, which is more convenient that the salt plates that need to be used in infrared spectroscopy. Because Raman spectroscopy involves the measurement of vibrational energy states with visible light, it is especially useful for measurements of vibrational processes that occur in the far IR portion of the spectrum. Finally, since Raman spectroscopy involves a scattering process, it can be used for remote monitoring such as atmospheric monitoring. A pulsed laser can be passed through the atmosphere or effluent from a smoke stack and Raman scattered radiation measured by remote detectors.

One disadvantage of Raman spectroscopy is that Raman scatter is an unfavorable process and the signals are weak compared to many other spectroscopic methods. There are two strategies that have been found to significantly increase the probability of Raman scatter and lower the detection limits.

One is a technique known as **surface-enhanced Raman spectroscopy (SERS)**. It is observed that compounds on surfaces consisting of roughened silver, gold or copper have much higher probability of producing Raman scatter. The other involves the use of **resonance Raman spectroscopy**. If the molecule is excited using a laser line close to an electronic absorption band, large enhancements in the Raman bands of symmetrical vibrations occur. As noted earlier, the lifetime of 10^{-14} second of Raman scatter indicates that the increased signal is not from a fluorescent transition.

This page titled 1.5: Raman Spectroscopy is shared under a CC BY-NC 4.0 license and was authored, remixed, and/or curated by Thomas Wenzel via source content that was edited to the style and standards of the LibreTexts platform.

- 5: Raman Spectroscopy by Thomas Wenzel is licensed CC BY-NC 4.0. Original source: https://asdlib.org/activelearningmaterials/molecular-and-atomic-spectroscopy.

1.6: Atomic Spectroscopy

Learning Objectives

After completing this unit the student will be able to:

- Compare and contrast the advantages of flame, furnace and inductively coupled plasma atomization sources.
- Justify why continuum radiation sources are usually not practical to use for atomic absorption spectroscopy.
- Describe the design of a hollow cathode lamp and justify the reasons for a hollow cathode configuration and low pressure of argon filler gas.
- Devise an instrumental procedure to account for flame noise in atomic absorption spectroscopy.
- Devise an instrumental procedure to account for molecular absorption and scatter from particulate matter in atomic absorption spectroscopy.
- Describe three possible strategies that can be used to overcome the problem of nonvolatile metal complexes.
- Devise a procedure to overcome excessive ionization of an analyte.
- Devise a procedure to account for matrix effects.

It is likely that most people studying chemistry have seen a demonstration where a solution of a metal salt was sprayed into a Bunsen burner and gave off a color that depended on the particular metal in the salt. Metal salts are used to create the different colors observed in firework displays. Analysis of the emission from the flame using a device called a spectroscope would further show the characteristic line emission spectrum of the metal species. The atomic emission observed in the flame involves a process whereby the metal ions in the salt are converted into neutral, excited atoms. These atoms then emit electromagnetic radiation corresponding to valence electron transitions.

This page titled 1.6: Atomic Spectroscopy is shared under a CC BY-NC 4.0 license and was authored, remixed, and/or curated by Thomas Wenzel via source content that was edited to the style and standards of the LibreTexts platform.

- 6: Atomic Spectroscopy by Thomas Wenzel is licensed CC BY-NC 4.0. Original source: https://asdlib.org/activelearningmaterials/molecular-and-atomic-spectroscopy.

1.7: Supplemental NMR Topics

Nuclear spin may be related to the nucleon composition of a nucleus in the following manner:

- Odd mass nuclei (i.e. those having an odd number of nucleons) have fractional spins.
  - Examples are I = 1/2 (^{1}H, ^{13}C, ^{19}F), I = 3/2 (^{11}B) & I = 5/2 (^{17}O).
- Even mass nuclei composed of odd numbers of protons and neutrons have integral spins. Examples are I = 1 (^{2}H, ^{14}N).
- Even mass nuclei composed of even numbers of protons and neutrons have zero spin (I = 0). Examples are ^{12}C, and ^{16}O.

Spin Properties of Nuclei

Spin 1/2 nuclei have a spherical charge distribution, and their NMR behavior is the easiest to understand. Other spin nuclei have nonspherical charge distributions and may be analyzed as prolate or oblate spinning bodies. All nuclei with non-zero spins have magnetic moments (**μ**), but the nonspherical nuclei also have an electric **quadrupole moment** (**eQ**). Some characteristic properties of selected nuclei are given in the following table.

Isotope	Natural % Abundance	Spin (I)	Magnetic Moment (μ)*	Magnetogyric Ratio (γ)†
^{1}H	99.9844	1/2	2.7927	26.753
^{2}H	0.0156	1	0.8574	4,107
^{11}B	81.17	3/2	2.6880	--
^{13}C	1.108	1/2	0.7022	6,728
^{17}O	0.037	5/2	-1.8930	-3,628
^{19}F	100.0	1/2	2.6273	25,179
^{29}Si	4.700	1/2	-0.5555	-5,319
^{31}P	100.0	1/2	1.1305	10,840

*** μ in units of nuclear magnetons = $5.05078 \cdot 10^{-27}$ JT^{-1}**
† γ in units of 10^{7} $rad\ T^{-1}\ sec^{-1}$

A Model for NMR Spectroscopy

The model of a spinning nuclear magnet aligned with or against an external magnetic field (for I = 1/2 nuclei) must be refined for effective interpretation of NMR phenomena. Just as a spinning mass will precess in a gravitational field (a gyroscope), the magnetic moment **μ** associated with a spinning spherical charge will precess in an external magnetic field. In the following illustration, the spinning nucleus has been placed at the origin of a cartesian coordinate system, and the external field is oriented along the z-axis. The frequency of precession is proportional to the strength of the magnetic field, as noted by the equation: $\omega_o = \gamma B_o$. The frequency ω_o is called the **Larmor frequency** and has units of radians per second. The proportionality constant **γ** is known as the **gyromagnetic ratio** and is proportional to the magnetic moment (**γ = 2pm/hI**). Some characteristic γ's were listed in the preceding table of nuclear properties.

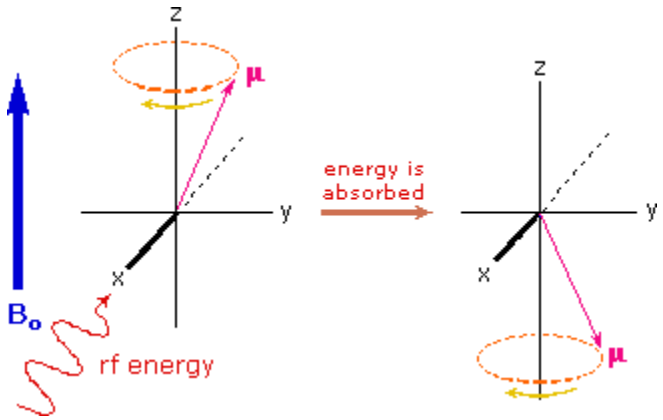


A Spinning Gyroscope in a Gravity Field

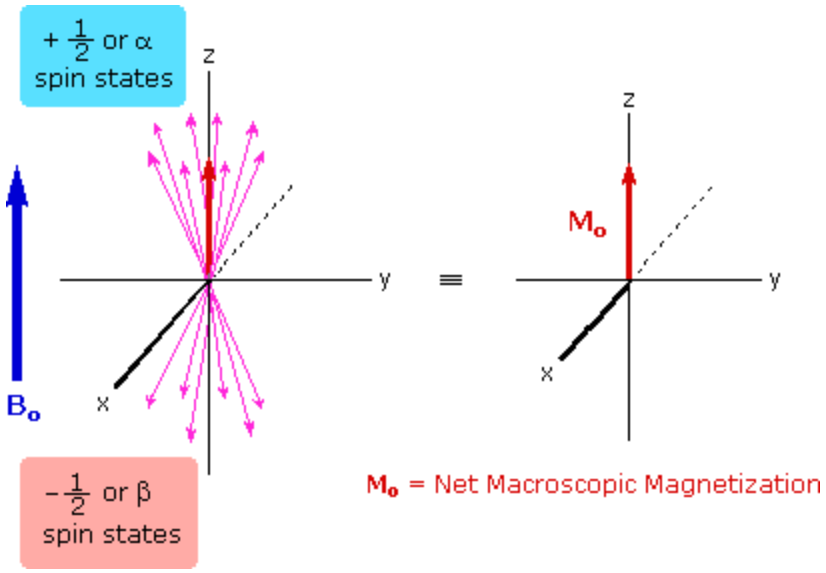
magnetic moment
μ

A Spinning Charge in a Magnetic Field

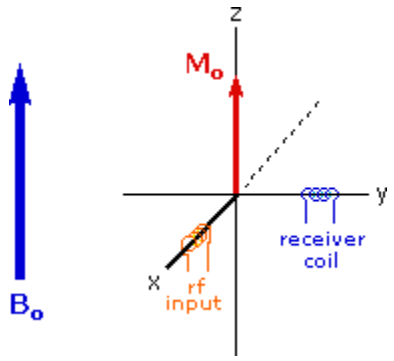
If rf energy having a frequency matching the Larmor frequency is introduced at a right angle to the external field (e.g. along the x-axis), the precessing nucleus will absorb energy and the magnetic moment will flip to its I = ⁻1/2 state. This excitation is shown in the following diagram. Note that frequencies in radians per second may be converted to Hz (cps) by dividing by 2π.



The energy difference between nuclear spin states is small compared with the average kinetic energy of room temperature samples, and the +1/2 and ⁻1/2 states are nearly equally populated. Indeed, in a field of 2.34 T the excess population of the lower energy state is only six nuclei per million. Although this is a very small difference , when we consider the number of atoms in a practical sample (remember the size of Avogadro's number), the numerical excess in the lower energy state is sufficient for selective and sensitive spectroscopic measurements. The diagram on the left below illustrates the macroscopic magnetization of a sample containing large numbers of spin 1/2 nuclei at equilibrium in a strong external magnetic field (B_o). A slight excess of +1/2 spin states precess randomly in alignment with the external field and a smaller population of ⁻1/2 spin states precess randomly in an opposite alignment. An overall net magnetization therefore lies along the z-axis.



Net Macroscopic Magnetization of a Sample in an External Magnetic Field B_0



Excitation by RF Energy and Subsequent Relaxation

The diagram and animation on the right show the changes in net macroscopic magnetization that occur as energy is introduced by rf irradiation at right angles to the external field. It is convenient to show the rf transmitter on the x-axis and the receiver-detector coil on the y-axis. On clicking the "Introduce RF Energy" button the animation will begin, and will repeat five times.

- First, the net magnetization shifts away from the z-axis and toward the y-axis. This occurs because some of the +1/2 nuclei are excited to the ⁻1/2 state, and the precession about the z-axis becomes coherent (non-random), generating a significant y component to the net magnetization (**M**). The animation pauses at this stage.
- After irradiation the nuclear spins return to equilibrium in a process called **relaxation**. As the xy coherence disappears and the population of the +1/2 state increases, energy is released and detected by the receiver. The net magnetization spirals back, and eventually the equilibrium state is reestablished.

An inherent problem of the NMR experiment must be pointed out here. We have noted that the population difference between the spin states is proportionally very small. A fundamental requirement for absorption spectroscopy is a population imbalance between a lower energy ground state and a higher energy excited state. This can be expressed by the following equation, where **A** is a proportionality constant. If the mole fractions of the spin states are equal ($\eta_+ = \eta_-$) then the population difference is zero and no absorption will occur. If the rf energy used in an NMR experiment is too high this **saturation** of the higher spin state will result and useful signals will disappear.

$$\text{Probability of Absorption} = A \times \rho(\nu_o) \times (\eta_+ - \eta_-)$$

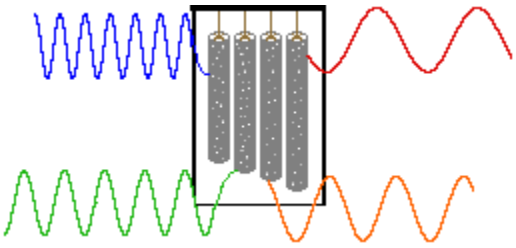
$\rho(\nu_o)$: radiation flux; $(\eta_+ - \eta_-)$: population imbalance

Relaxation Mechanisms

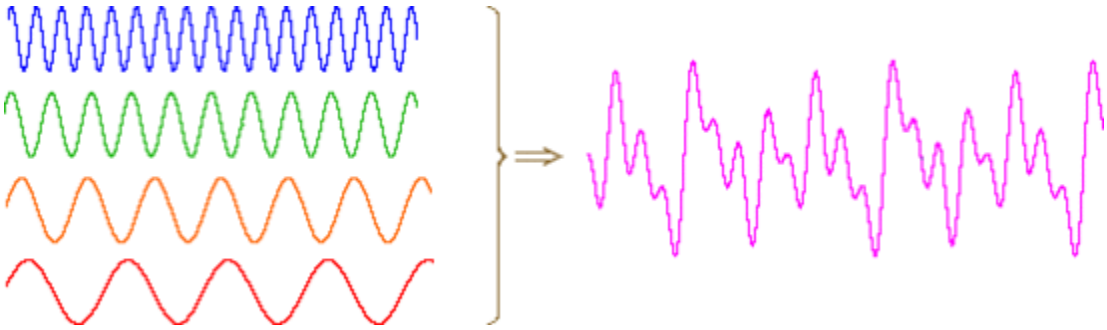
For NMR spectroscopy to be practical, an efficient mechanism for nuclei in the higher energy $^{-}1/2$ spin state to return to the lower energy +1/2 state must exist. In other words, the spin population imbalance existing at equilibrium must be restored if spectroscopic observations are to continue. Now an isolated spinning nucleus will not spontaneouly change its spin state in the absence of external perturbation. Indeed, hydrogen gas (H_2) exists as two stable spin isomers: ortho (parallel proton spins) and para (antiparallel spins). NMR spectroscopy is normally carried out in a liquid phase (solution or neat) so that there is close contact of sample molecules with a rapidly shifting crowd of other molecules (Brownian motion). This thermal motion of atoms and molecules generates local fluctuating electromagnetic fields, having components that match the Larmor frequency of the nucleus being studied. These local fields stimulate emission/absorption events that establish spin equilibrium, the excess spin energy being detected as it is released. This relaxation mechanism is called **Spin-Lattice Relaxation** (or Longitudinal Relaxation). The efficiency of spin-lattice relaxation depends on factors that influence molecular movement in the lattice, such as viscosity and temperature. The relaxation process is kinetically first order, and the reciprocal of the rate constant is a characteristic variable designated $\mathbf{T_1}$, the spin-lattice relaxation time. In non-viscous liquids at room temperature T_1 ranges from 0.1 to 20 sec. A larger T_1 indicates a slower or more inefficient spin relaxation. Another relaxation mechanism called spin-spin relaxation (or transverse relaxation) is characterized by a relaxation time T_2. This process, which is actually a spin exchange, will not be discussed here.

Pulsed Fourier Transform Spectroscopy

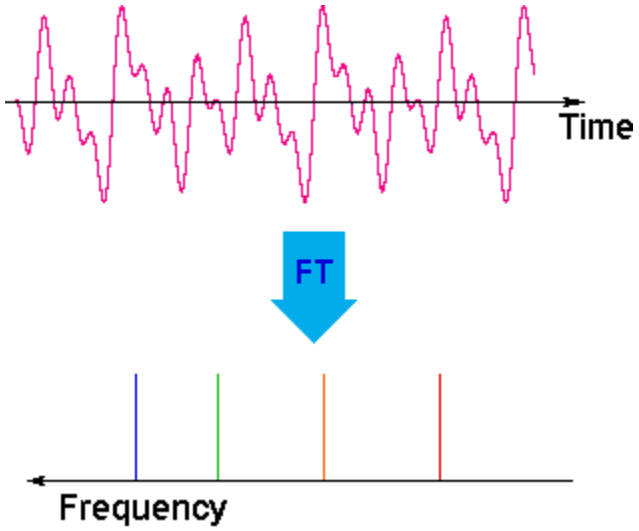
In a given strong external magnetic field, each structurally distinct set of hydrogens in a molecule has a characteristic resonance frequency, just as each tubular chime in percussion instrument has a characteristic frequency. To discover the frequency of a chime we can strike it with a mallet and measure the sound emitted. This procedure can be repeated for each chime in the group so that all the characteristic frequencies are identified.



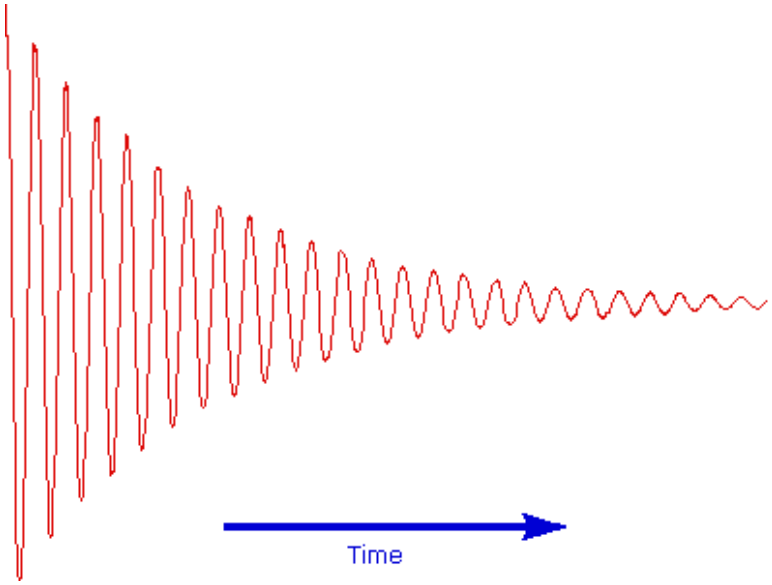
An alternative means of aquiring the same information is to strike all the chimes simultaneously, and to subject the complex collection of frequencies produced to mathematical analysis. In the following diagram the four frequencies assigned to our set of chimes are added together to give a complex summation wave. This is a straightforward conversion; and the reverse transformation, while not as simple, is readily accomplished, provided the combination signal is adequately examined and characterized.



A CW NMR spectrometer functions by irradiating each set of distinct nuclei in turn, a process analagous to striking each chime independently. For a high resolution spectrum this must be done slowly, and a 12 ppm sweep of the proton region takes from 5 to 10 minutes. It has proven much more efficient to excite all the proton nuclei in a molecule at the same time, followed by mathematical analysis of the complex rf resonance frequencies emitted as they relax back to the equilibrium state. This is the principle on which a pulse Fourier transform spectrometer operates. By exposing the sample to a very short (10 to 100 μsec), relatively strong (about 10,000 times that used for a CW spectrometer) burst of rf energy along the x-axis, as described above, all of the protons in the sample are excited simultaneously. The macroscopic magnetization model remains useful if we recognize it is a combination of megnetization vectors for all the nuclei that have been excited.



The overlapping resonance signals generated as the excited protons relax are collected by a computer and subjected to a Fourier transform mathematical analysis. As shown in the diagram on the left, the Fourier transform analysis, abbreviated FT, converts the complex time domain signal emitted by the sample into the frequency (or field) domain spectrum we are accustomed to seeing. In this fashion a complete spectrum can be acquired in a few seconds. Because the relaxation mechanism is a first order process, the rf signal emitted by the sample decays exponentially. This is called a **free induction decay** signal, abbreviated **FID**.



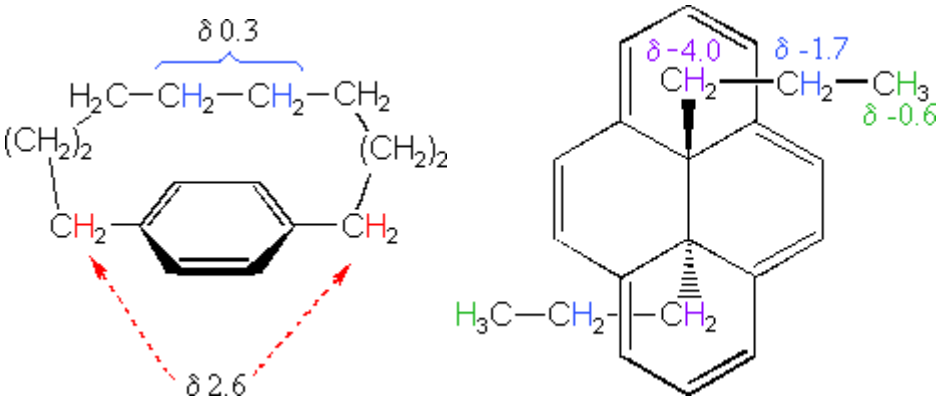
Free Induction Decay Signal

Since, the FID signal collected after one pulse, may be stored and averaged with the FID's from many other identical pulses prior to the Fourier transform, the NMR signal strength from a small sample may be enhanced to provide a useable spectrum. This has been essential to acquiring spectra from low abundance isotopes, such as ^{13}C. In practice, the pulse FT experiment has proven

so versatile that many variations of the technique, suited to special purposes, have been devised and used effectively.

Examples of Anisotropy Influences on Chemical Shift

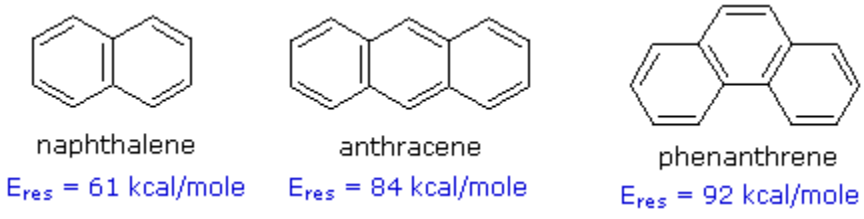
The compound on the left has a chain of ten methylene groups linking para carbons of a benzene ring. Such bridged benzenes are called **paracyclophanes**. The meta analogs are also known. The structural constraints of the bridging chain require the middle two methylene groups to lie over the face of the benzene ring, which is a NMR shielding region. The four hydrogen atoms that are part of these groups display resonance signals that are more than two ppm higher field than the two methylene groups bonded to the edge of the ring (a deshielding region).



The 14 π-electron bridged annulene on the right is an aromatic (4n + 2) system, and has the same anisotropy as benzene. Nuclei located over the face of the ring are shielded, and those on the periphery are deshielded. The ring hydrogens give resonance signals in the range 8.0 to 8.7 δ, as expected from their deshielded location (note that there are three structurally different hydrogens on the ring). The two propyl groups are structurally equivalent (homotopic), and are free to rotate over the faces of the ring system (one above and one below). On average all the propyl hydrogens are shielded, with the innermost methylene being the most affected. The negative chemical shifts noted here indicate that the resonances occurs at a higher field than the TMS reference signal.

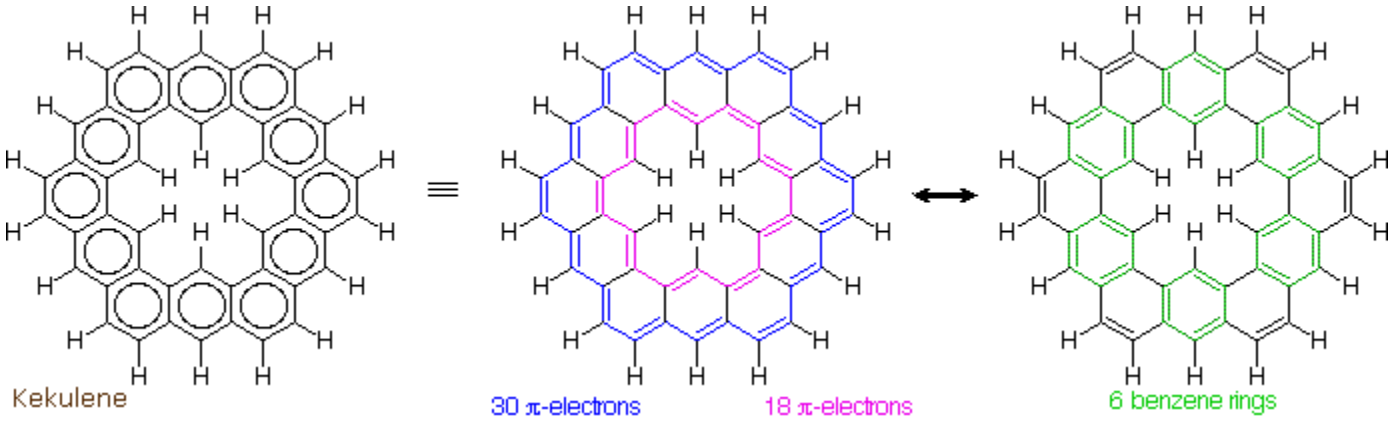
A remarkable characteristic of annulenes is that antiaromatic 4n π-electron systems are anisotropic in the opposite sense as their aromatic counterparts. A dramatic illustration of this fact is provided by the dianion derivative of the above bridged annulene. This dianion, formed by the addition of two electrons, is a 16 π-electron (4n) system. In the NMR spectrum of the dianion, the ring hydrogens resonate at high field (they are shielded), and the hydrogens of the propyl group are all shifted downfield (deshielded). The innermost methylene protons (magenta) give an NMR signal at +22.2 ppm, and the signals from the adjacent methylene and methyl hydrogens also have unexpectedly large chemical shifts.

Compounds in which two or more benzene rings are fused together include examples such as naphthalene, anthracene and phenanthrene, shown in the following diagram, present interesting insights into aromaticity and reactivity. The resonance stabilization of these compounds, calculated from heats of hydrogenation or combustion, is given beneath each structure.



Unlike benzene, the structures of these compounds show measurable double bond localization, which is reflected in their increased reactivity both in substitution and addition reactions. However, the ^{1}HNMR spectra of these aromatic hydrocarbons do not provide much insight into the distribution of their pi-electrons. As expected, naphthalene displays two equally intense signals at δ 7.46 & 7.83 ppm. Likewise, anthracene shows three signals, two equal intensity multiplets at δ 7.44 & 7.98 ppm and a signal half as intense at δ 8.4 ppm. Thus, the influence of double bond localization or competition between benzene and higher annulene stabilization cannot be discerned.

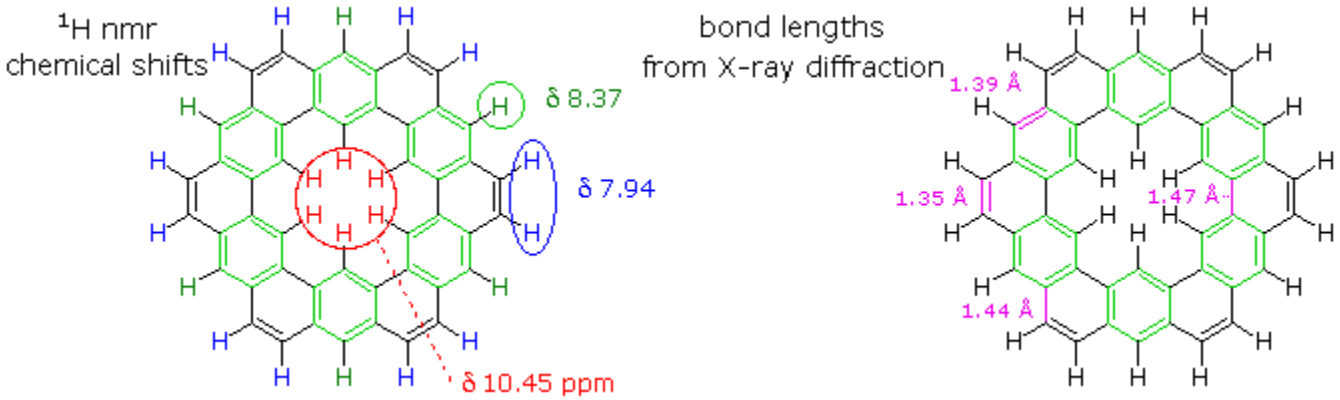
The much larger $C_{48}H_{24}$ fused benzene ring cycle, named "kekulene" by Heinz Staab and sometimes called "superbenzene" by others, serves to probe the relative importance of benzenoid versus annulenoid aromaticity. A generic structure of this remarkable compound is drawn on the left below, together with two representative Kekule contributing structures on its right. There are some 200 Kekule structures that can be drawn for kekulene, but these two canonical forms represent extremes in aromaticity. The central formula has two [4n+2] annulenes, an inner [18]annulene and an outer [30]annulene (colored pink and blue respectively). The formula on the right has six benzene rings (colored green) joined in a ring by meta bonds, and held in a planar configuration by six cis-double bond bridges.



The coupled annulene contributor in the center has an energetically equivalent canonical form in which the single and double bonds making up the annulenes are exchanged. If these contributors dominate the aromatic character of kekulene, the 6 inside hydrogens should be shielded by the ring currents, and the 18 hydrogens on the periphery should be deshielded. Furthermore, the C:C bonds composing each annulene ring should have roughly equal lengths.

If the benzene contributor on the right (and its equivalent Kekule form) dominate the aromaticity of kekulene, all the benzene hydrogens will be deshielded, and the six double bond links on the periphery will have bond lengths characteristic of fixed single and double bonds

The extreme insolubility of kekulene made it difficult to grow suitable crystals for X-ray analysis or obtain solution NMR spectra. These problems were eventually solved by using high boiling solvents, the ^{1}HNMR spectrum being taken at 150 to 200° C in deuterated tetrachlorobenzene solution. The experimental evidence demonstrates clearly that the hexa-benzene ring structure on the right most accurately represents kekulene. This evidence is shown below. The extremely low field resonance of the inside hydrogens is assigned from similar downfield shifts in model compounds.

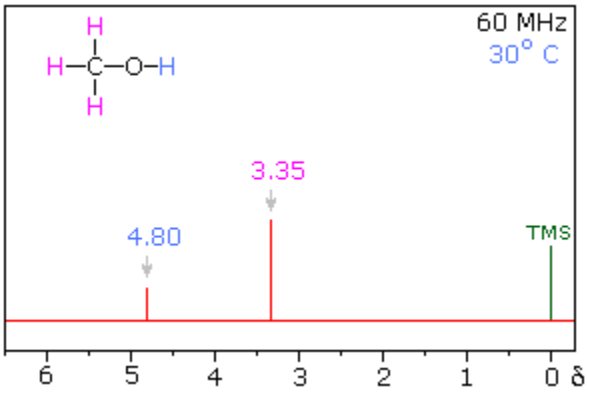


It is important to understand that the **shielding** and **deshielding** terms used throughout our discussion of relative chemical shifts are themselves **relative**. Indeed, compared to a hypothetical isolated proton, all the protons in a covalent compound are shielded by the electrons in nearby sigma and pi-bonds. Consequently, it would be more accurate to describe chemical shift differences in terms of the absolute shielding experienced by different groups of hydrogens. There is, in fact, good evidence that the anisotropy

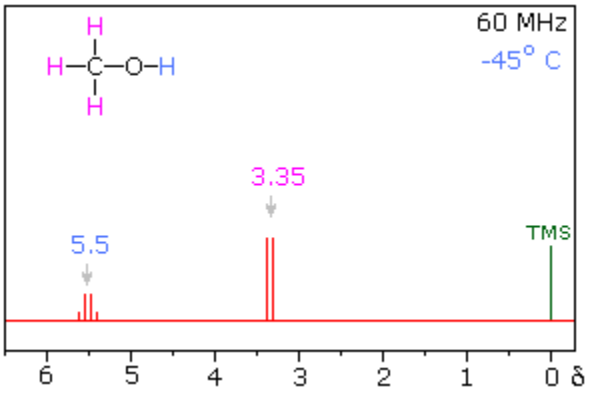
of neighboring C-H and C-C sigma bonds, together with that of the bond to the observed hydrogen, are the dominate shielding factors influencing chemical shifts. The anisotropy of pi-electron systems augments this sigma skeletal shielding. Nevertheless, the deceptive focus on anisotropic pi-electron influences is so widely and commonly used that this view has been retained and employed in these pages.

Hydrogen Bonding Influences

Hydrogen bonding of hydroxyl and amino groups not only causes large variations in the chemical shift of the proton of the hydrogen bond, but also influences its coupling with adjacent C-H groups. As shown on the right, the 60 MHz proton NMR spectrum of pure (neat) methanol exhibits two signals, as expected. At 30° C these signals are sharp singlets located at δ 3.35 and 4.80 ppm, the higher-field methyl signal (magenta) being three times as strong as the OH signal (orange) at lower field. When cooled to -45 ° C, the larger higher-field signal changes to a doublet (J = 5.2 Hz) having the same chemical shift. The smaller signal moves downfield to δ 5.5 ppm and splits into a quartet (J = 5.2 Hz). The relative intensities of the two groups of signals remains unchanged. This interesting change in the NMR spectrum, which is shown in the two spectra below, is due to increased stability of hydrogen bonded species at lower temperature. Since hydrogen bonding not only causes a resonance shift to lower field, but also decreases the rate of intermolecular proton exchange, the hydroxyl proton remains bonded to the alkoxy group for a sufficient time to exert its spin coupling influence.
Under routine conditions, rapid intermolecular exchange of the OH protons of alcohols often prevents their coupling with adjacent hydrogens from being observed. Intermediate rates of proton exchange lead to a broadening of the OH and coupled hydrogen signals, a characteristic that is useful in identifying these functions. Since traces of acid or base catalyze this hydrogen exchange, pure compounds and clean sample tubes must be used for experiments of the kind described here.



Methanol ^{1}H NMR at approximately Room Temperature



Methanol ^{1}H NMR at -45 ^{o}C

Another way of increasing the concentration of hydrogen bonded methanol species is to change the solvent from chloroform-d to a solvent that is a stronger hydrogen bond acceptor. Examples of such solvents are given in the following table. In contrast to

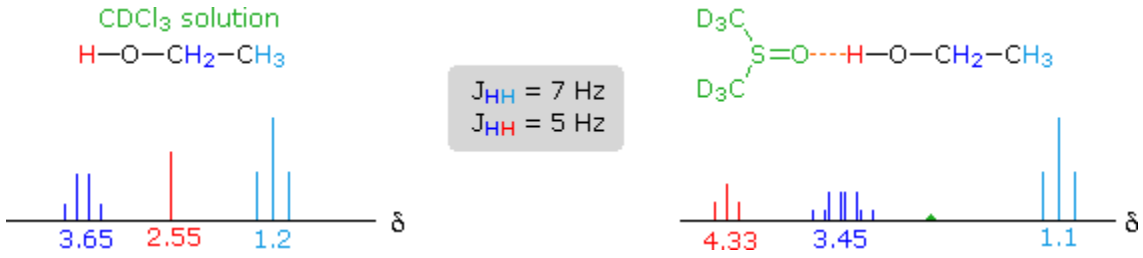
the neat methanol experiment described above, very dilute solutions are used for this study. Since chloroform is a poor hydrogen bond acceptor and the dilute solution reduces the concentration of methanol clusters, the hydroxyl proton of methanol generates a resonance signal at a much higher field than that observed for the pure alcohol. Indeed, the OH resonance signal from simple alcohols in dilute chloroform solution is normally found near δ 1.0 ppm.

The exceptionally strong hydrogen bond acceptor quality of DMSO is demonstrated here by the large downfield shift of the methanol hydroxyl proton, compared with a slight upfield shift of the methyl signal. The expected spin coupling patterns shown above are also observed in this solvent. Although acetone and acetonitrile are better hydrogen-bond acceptors than chloroform, they are not as effective as DMSO.

^{1}H Chemical Shifts of Methanol in Selected Solvents

Solvent	$CDCl_3$	CD_3COCD_3	CD_3SOCD_3	$CD_3C{\equiv}N$
CH_3–O–H **CH_3** **O–H**	3.40 1.10	3.31 3.12	3.16 4.01	3.28 2.16

The solvent effect shown above suggests a useful diagnostic procedure for characterizing the OH resonance signals from alcohol samples. For example, a solution of ethanol in chloroform-d displays the spectrum shown on the left below, especially if traces of HCl are present (otherwise broadening of the OH and CH_2 signals occurs). Note that the chemical shift of the OH signal (red) is less than that of the methylene group (blue), and no coupling of the OH proton is apparent. The vicinal coupling (J = 7 Hz) of the methyl and methylene hydrogens is typical of ethyl groups. In DMSO-d_6 solution small changes of chemical shift are seen for the methyl and methylene group hydrogens, but a dramatic downfield shift of the hydroxyl signal takes place because of hydrogen bonding. Coupling of the OH proton to the adjacent methylene group is evident, and both the coupling constants can be measured. Because the coupling constants are different, the methylene signal pattern is an overlapping doublet of quartets (eight distinct lines) rather than a quintet. Note that residual hydrogens in the solvent give a small broad signal near δ 2.5 ppm.

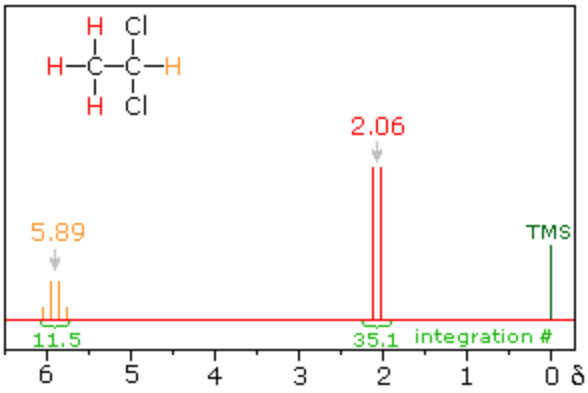


For many alcohols in dilute chloroform-d solution, the hydroxyl resonance signal is often broad and obscured by other signals in the δ 1.5 to 3.0 region. The simple technique of using DMSO-d_6 as a solvent, not only shifts this signal to a lower field, but permits 1°-, 2 °- & 3 °-alcohols to be distinguished. Thus, the hydroxyl proton of 2-propanol generates a doublet at δ 4.35 ppm, and the corresponding signal from 2-methyl-2-propanol is a singlet at δ 4.2 ppm. The more acidic OH protons of phenols are similarly shifted – from δ 4 to 7 in chloroform-d to δ 8.5 to 9.5 in DMSO-d_6.

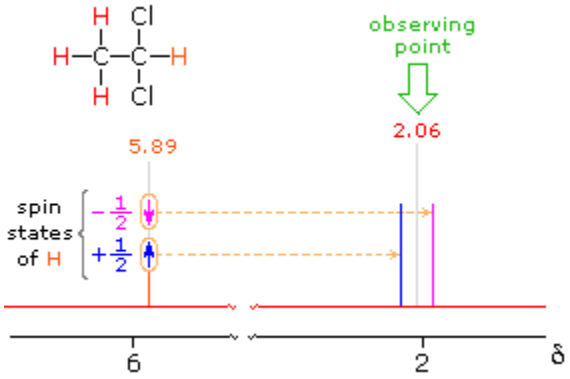
Spin-Spin Coupling

vicinal (joined by three sigma bonds). In this case a neighboring proton having a +1/2 spin shifts the resonance frequency of the proton being observed to a slightly higher value (up to 7 Hz), and a -1/2 neighboring spin shifts it to a lower frequency. Remember that the total population of these two spin states is roughly equal, differing by only a few parts per million in a strong magnetic field. If several neighboring spins are present, their effect is additive.

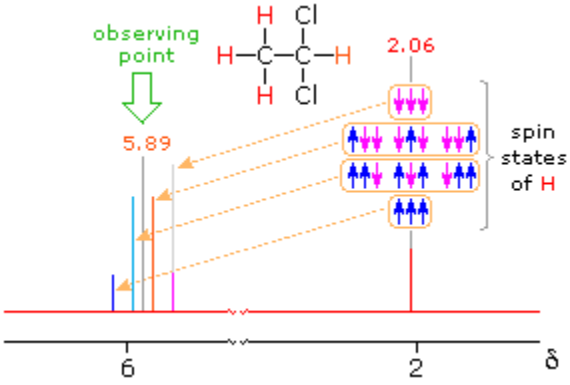
In the spectrum of 1,1-dichloroethane shown on the right, it is clear that the three methyl hydrogens (red) are coupled with the single methyne hydrogen (orange) in a manner that causes the former to appear as a doublet and the latter as a quartet. The light gray arrow points to the unperturbed chemical shift location for each proton set. By clicking on one of these signals, the spin relationship that leads to the coupling pattern will be displayed. Clicking elsewhere in the picture will return the original spectrum.



Full Spectrum of 1,1-dichloroethane

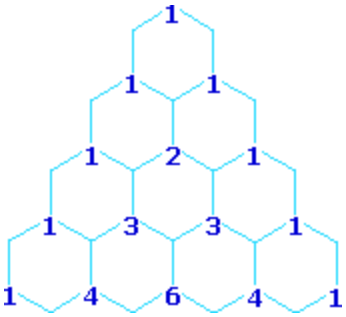


2.06 ppm Signal Explained



5.89 ppm Signal Explained

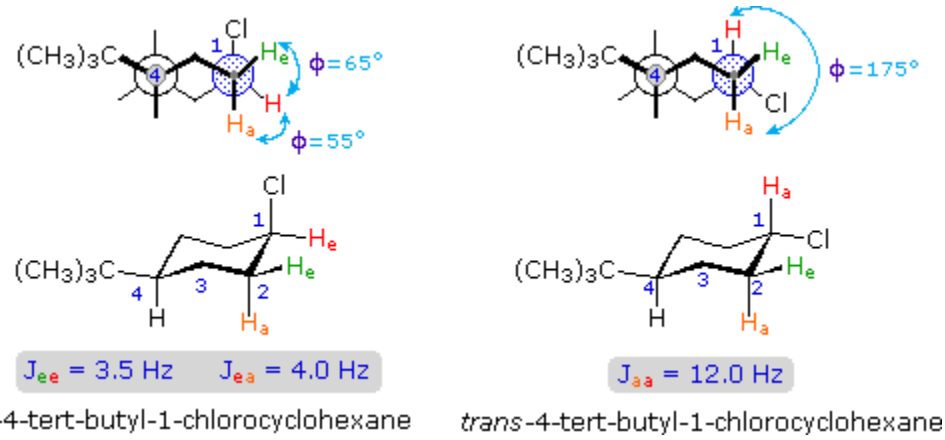
The statistical distribution of spins within each set explains both the n+1 rule and the relative intensities of the lines within a splitting pattern. The action of a single neighboring proton is easily deduced from the fact that it must have one of two possible spins. Interaction of these two spin states with the nuclei under observation leads to a doublet located at the expected chemical shift. The corresponding action of the three protons of the methyl group requires a more detailed analysis. In the display of this interaction four possible arrays of their spins are shown. The mixed spin states are three times as possible as the all +1/2 or all ⁻1/2 collection. Consequently, we expect four signals, two above the chemical shift and two below it. This spin analysis also suggests that the intensity ratio of these signals will be 1:3:3:1. The line separations in splitting patterns are measured in Hz, and are characteristic of the efficiency of the spin interaction; they are referred to as coupling constants (symbol J). In the above example, the common coupling constant is 6.0 Hz.



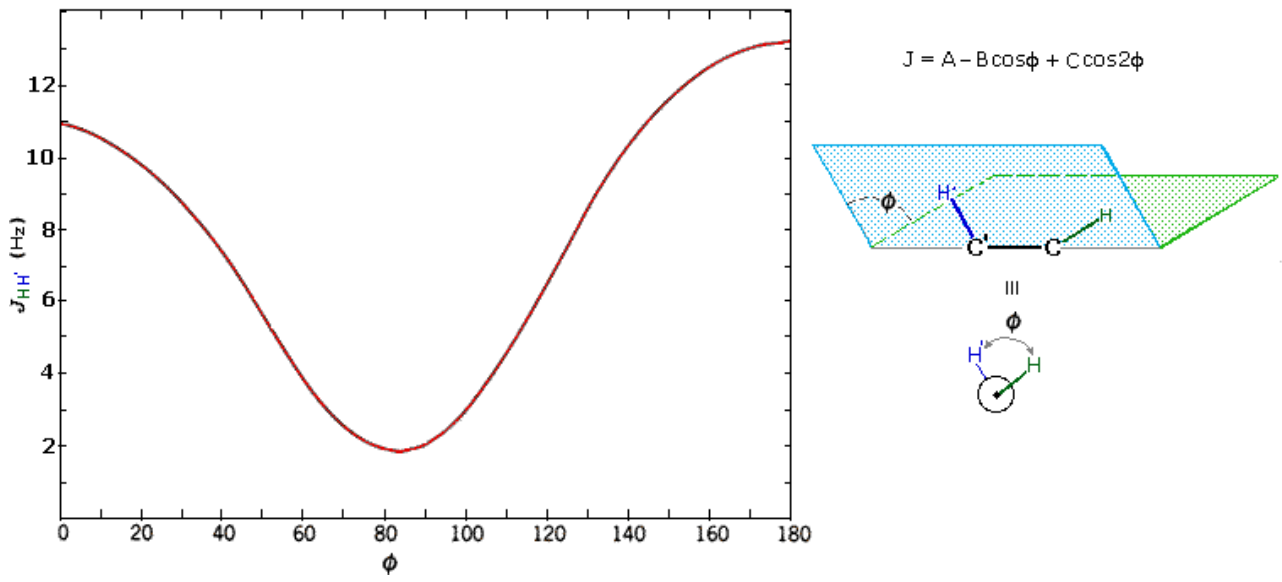
Multiplitiicy Relative Line Intensity (Starting at the top: Singlet, Doublet, Triplet, Quartet, and Quintet)

A simple way of estimating the relative intensities of the lines in a first-order coupling pattern is shown on the right. This array of numbers is known as Pascal's triangle, and is easily extended to predict higher multiplicities. The number appearing at any given site is the sum of the numbers linked to it from above by the light blue lines. Thus, the central number of the five quintet values is 3 + 3 = 6. Of course, a complete analysis of the spin distributions, as shown for the case of 1,1-dichloroethane above, leads to the same relative intensities.

Coupling constants are independent of the external magnetic field, and reflect the unique spin interaction characteristics of coupled sets of nuclei in a specific structure. As noted earlier, coupling constants may vary from a fraction of a Hz to nearly 20 Hz, important factors being the nature and spatial orientation of the bonds joining the coupled nuclei. In simple, freely rotating alkane units such as CH_3CH_2X or YCH_2CH_2X the coupling constant reflects an average of all significant conformers, and usually lies in a range of 6 to 8 Hz. This conformational mobility may be restricted by incorporating the carbon atoms in a rigid ring, and in this way the influence of the dihedral orientation of the coupled hydrogens may be studied.



The structures of cis and trans-4-tert-butyl-1-chlorocyclohexane, shown above, illustrate how the coupling constant changes with the dihedral angle (φ) between coupled hydrogens. The inductive effect of chlorine shifts the resonance frequency of the red colored hydrogen to a lower field (δ ca. 4.0), allowing it to be studied apart from the other hydrogens in the molecule. The preferred equatorial orientation of the large tert-butyl group holds the six-membered ring in the chair conformation depicted in the drawing. In the trans isomer this fixes the red hydrogen in an axial orientation; whereas for the cis isomer it is equatorial. The listed values for the dihedral angles and the corresponding coupling constants suggest a relationship, which has been confirmed and clarified by numerous experiments. This relationship is expressed by the **Karplus** equation shown below.

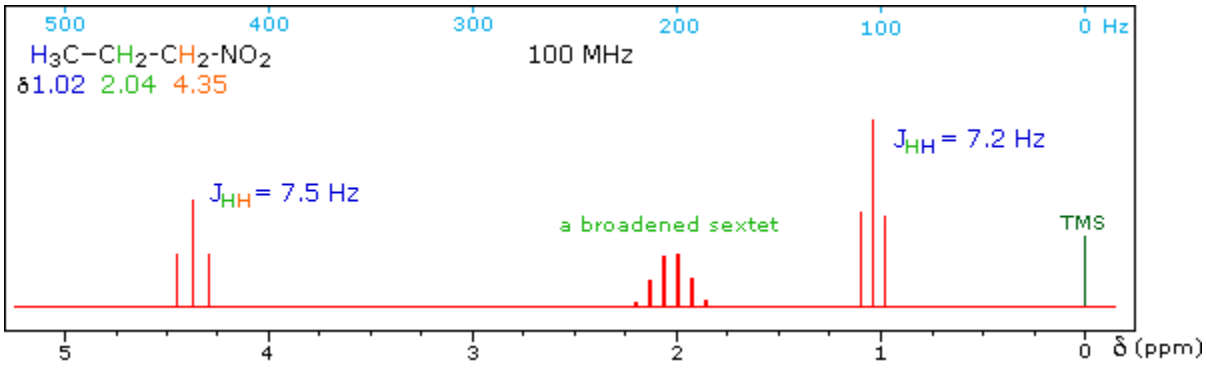


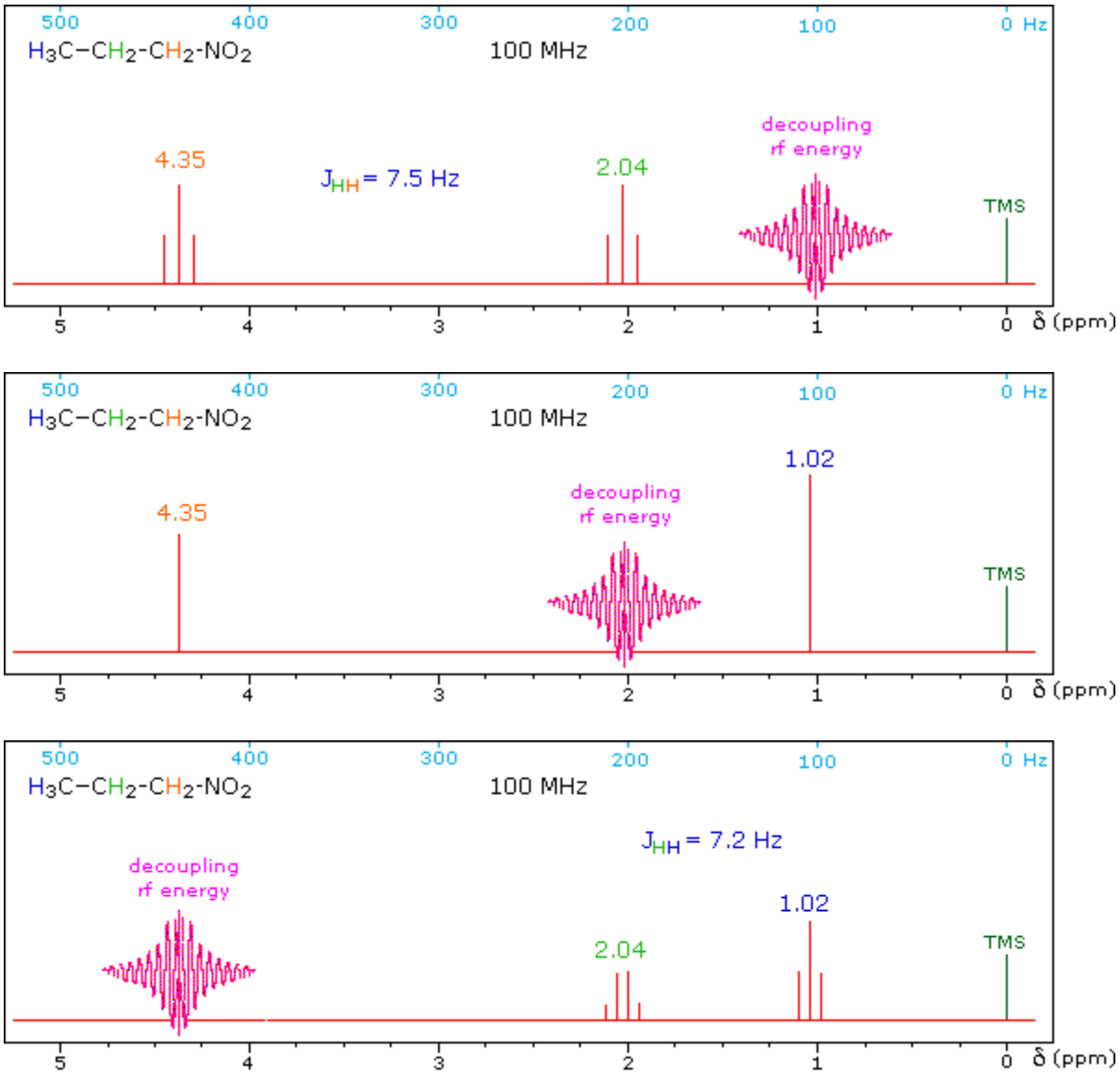
Geminal couplings are most commonly observed in cyclic structures, but are also evident when methylene groups have diastereomeric hydrogens.

Spin Decoupling

We have noted that rapidly exchanging hydroxyl hydrogens are not spin-coupled to adjacent C-H groups. The reason for this should be clear. As each exchange occurs, there will be an equal chance of the new proton having a +1/2 or a ⁻1/2 spin (remember that the overall populations of the two spin states are nearly identical). Over time, therefore, the hydroxyl hydrogen behaves as though it is rapidly changing its spin, and the adjacent nuclei see only a zero spin average from it. If we could cause other protons in a molecule to undergo a similar spin averaging, their spin-coupling influence on adjacent nuclei would cease. Such NMR experiments are possible, and are called **spin decoupling**.

When a given set of nuclei is irradiated with strong rf energy at its characteristic Larmor frequency, spin saturation and rapid interconversion of the spin states occurs. Neighboring nuclei with different Larmor frequencies are no longer influenced by specific long-lived spins, so spin-spin signal splitting of the neighbors vanishes. The following spectrum of 1-nitropropane may be used to illustrate this technique. The three distinct sets of hydrogens in this molecule generate three resonance signals (two triplets and a broad sextet). A carefully tuned decoupling signal may be broadcast into the sample while the remaining spectrum is scanned. The region of the decoupling signal is obscured, but resonance signals more than 60 Hz away may still be seen. By clicking on one of the three signals in the spectrum, the results of decoupling at that frequency will be displayed.





The Influence of Magnetic Field Strength

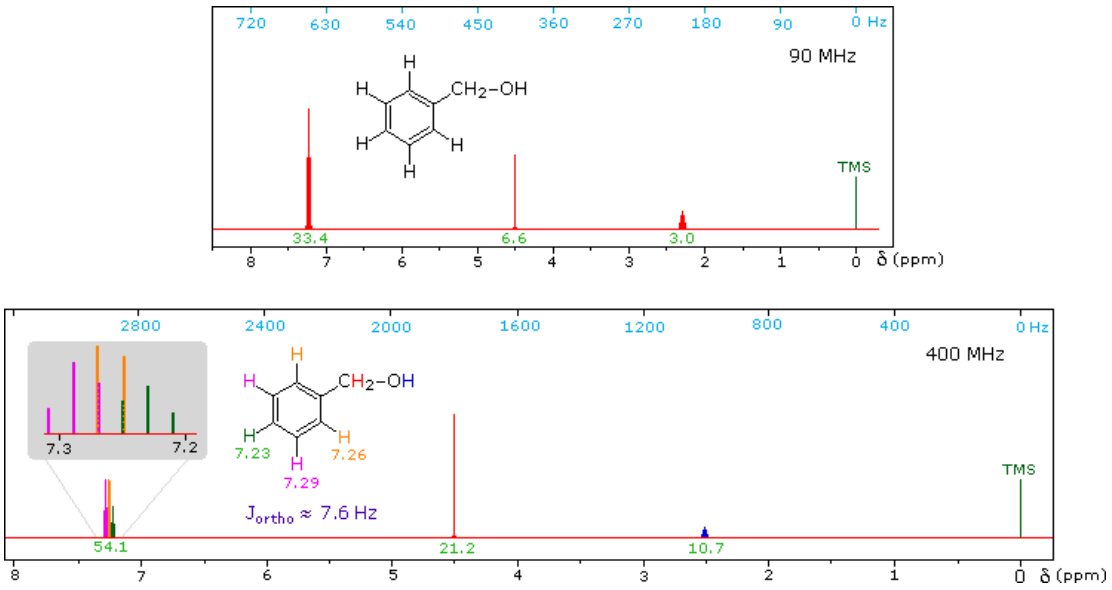
The presence of symmetrical, easily recognized first-order splitting patterns in a NMR spectrum depends on the relative chemical shifts of the spin-coupled nuclei and the magnitude of the coupling constant. If the chemical shift difference (i.e. $\Delta\delta$ in Hz) is large compared to J the splitting patterns will be nearly first order. If, on the other hand, the difference is relatively small (less than 10 J) second order distortion of the signal splitting will be observed. One important advantage in using very high field magnets for NMR is that the separation (or dipersion) of different sets of protons is proportional to field strength, whereas coupling constants do not change.

It is important to remember that structurally different sets of nuclei do not always produce distinctly different signals in an NMR spectrum. For example, the hydrocarbon octane has four different sets of protons, as shown in the following formula:

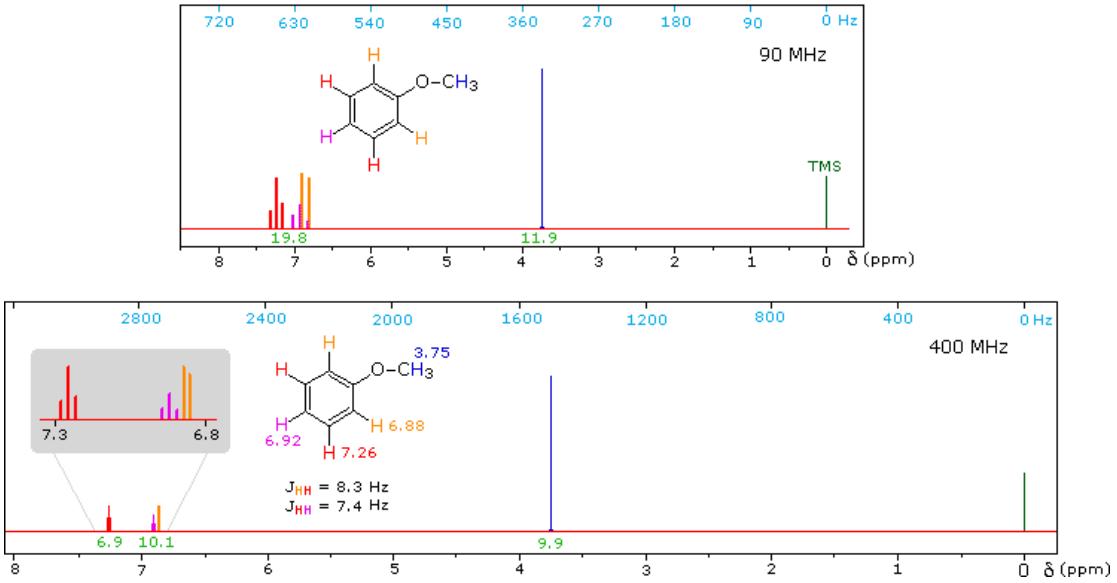
$CH_3CH_2CH_2CH_2CH_2CH_2CH_2CH_3$

Now methyl hydrogens have a smaller chemical shift than methylene hydrogens, so methyl groups (colored black here) can usually be distinguished. However, the chemical shifts of the different methylene groups (blue, red & green) are so similar that many NMR spectrometers will not resolve them. Consequently, a 90 MHz proton spectrum of octane shows a distorted triplet at δ 0.9 ppm, produced by the six methyl protons, and a strong broad singlet at δ 1.2 ppm coming from all twelve methylene protons. A similar failure to resolve structurally different hydrogen atoms occurs in the case of alkyl substituted benzene rings. The chemical shift difference between ortho, meta and para hydrogens in such compounds is often so small that they are seen as a single

resonance signal in an NMR spectrum. The 90 MHz spectrum of benzyl alcohol in chloroform-d solution provides an instructive example, shown below. A broad strong signal at δ 7.24 ppm is characteristic of the aromatic protons on alkylbenzenes. Since the chemical shifts of these hydrogens are nearly identical, no spin coupling is observed. If the magnetic field strength is increased to 400 Mz (lower spectrum) the aromatic protons are more dispersed (orange, magenta and green signals), and the spin coupling of adjacent hydrogens (J = 7.6 Hz) causes overlap of the signals (gray shaded enlargement).



^{1}H NMR of Benzyl alcohol



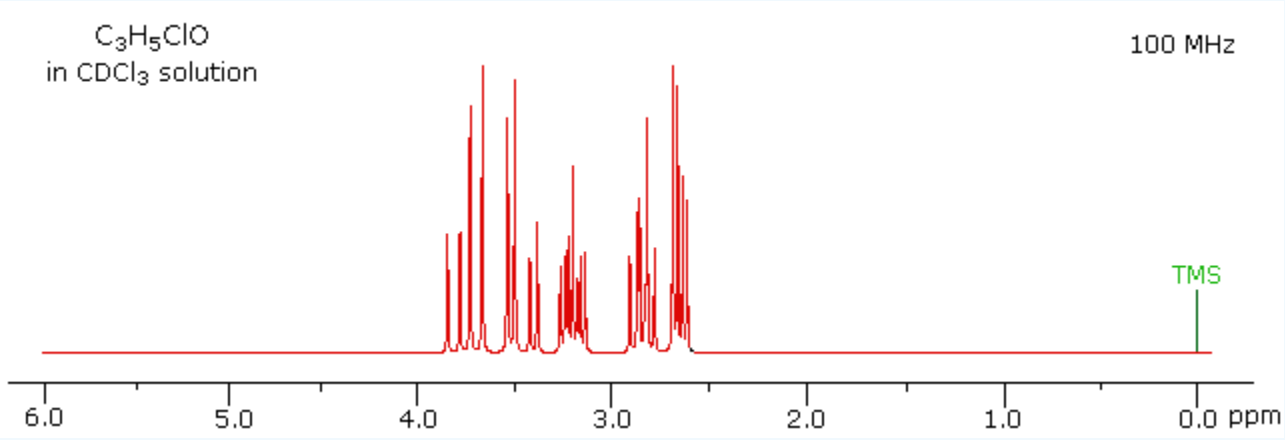
^{1}H NMR of Anisole

Anisole, an isomer of benzyl alcohol, has a more dispersed set of aromatic signals, thanks to the electron donating influence of the methoxy substituent. The 90 MHz spectrum of anisole shows this greater dispersion, but the spin coupling of adjacent hydrogens still results in signal overlap. The 400 Mz spectrum at the bottom illustrates the greater dispersion of the chemical shifts, and since the coupling constants remain unchanged, the splitting patterns no longer overlap. In all these examples a very small meta-hydrogen coupling has been ignored.

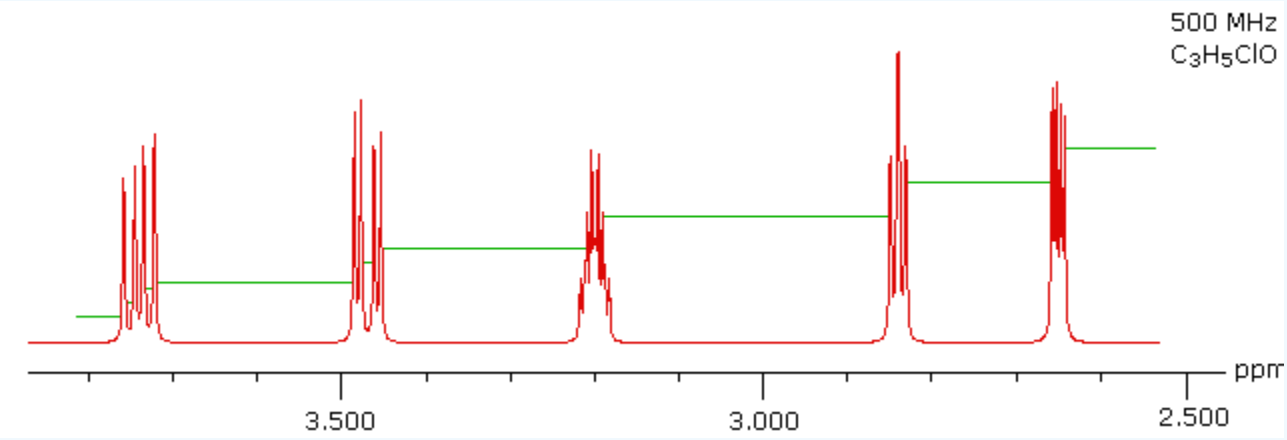
Example 1.7.1

Not all simple compounds have simple proton NMR spectra. The following example not only illustrates this point, but also demonstrates how a careful structural analysis can rationalize an initially complex spectrum.

The 100 MHz ^{1}H NMR spectrum of a C_3H_5ClO compound is initially displayed. This spectrum is obviously complex and not easily interpreted, except for concluding that no olefinic C-H protons are present.

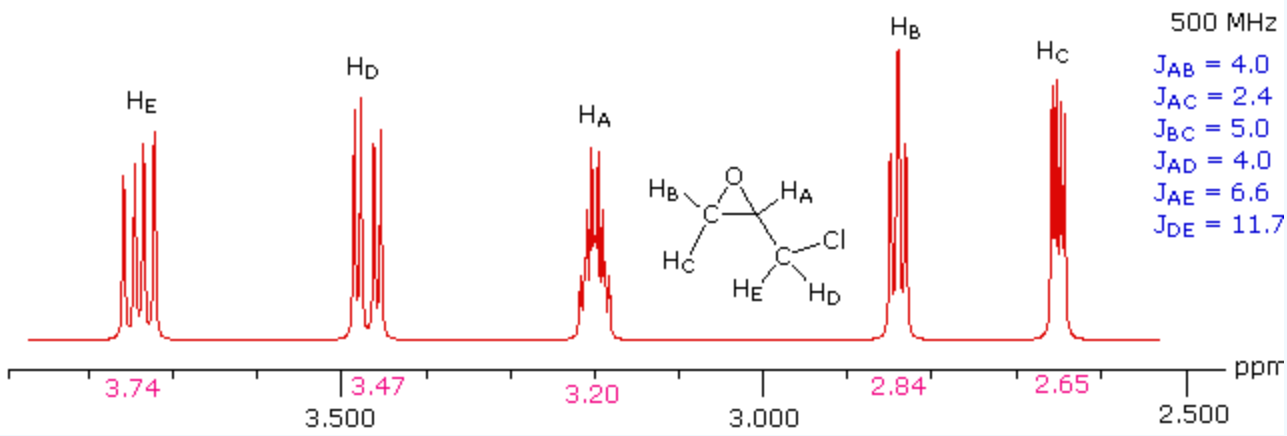


With a higher field spectrum it is clear that each of the five hydrogen atoms in the molecule is structurally unique, and is producing a separate signal. Also, it is clear there is considerable spin coupling of all the hydrogens. To see the coupling patterns more clearly it is necessary to expand and enhance the spectrum in these regions. For purposes of our demonstration, this can be done by clicking on any one of the signal multiplets. Clicking in an open area should return the original 500 MHz display. In some of the expanded displays two adjacent groups of signals are shown. Once an enlarged pattern is displayed, the line separations in Hz can be measured (remember that for a 500 MHz spectrum 1 ppm is 500 Hz). The middle signal at 3.2 ppm is the most complex, and overlap of some multiplet lines has occurred.

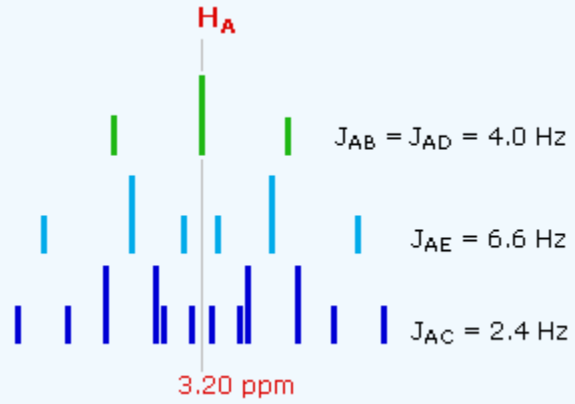


Solution

This spectrum has several interesting features. First, hydrogens A, B & C are clearly different, and are spin-coupled to each other. Hydrogens B & C are geminally related, whereas A is oriented to B & C in a vicinal manner. Since J_{AB} and J_{BC} are similar, the H_B signal is a broad triplet. Although hydrogens D & E might seem identical at first glance, they are diastereotopic, and should therefore have different chemical shifts. The DE geminal coupling constant is 11.7 Hz, so each of these hydrogens appears as a doublet of doublets.

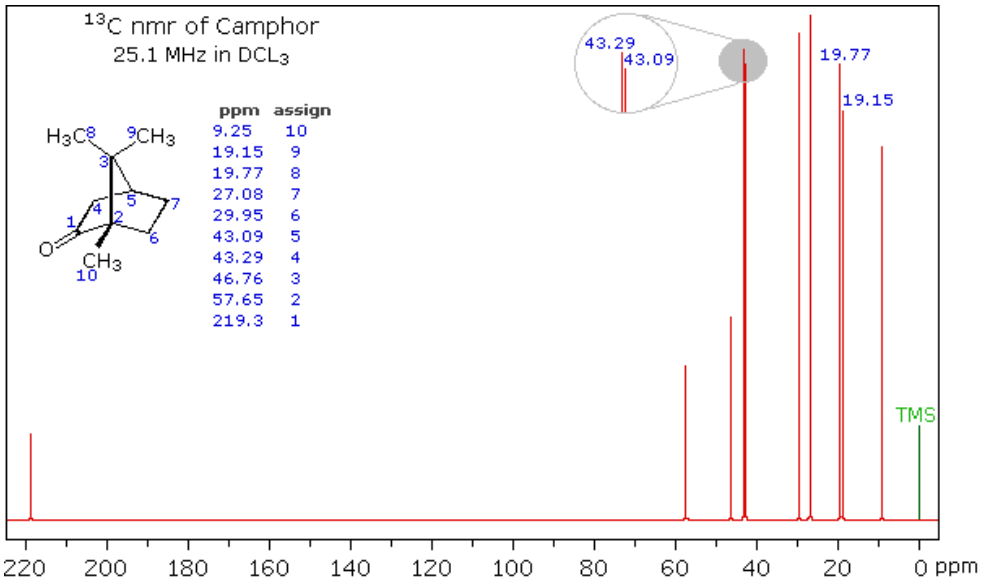


The splitting of the H_A signal is complex and not immediately obvious. The diagram shows the consequences of the four operating coupling constants.

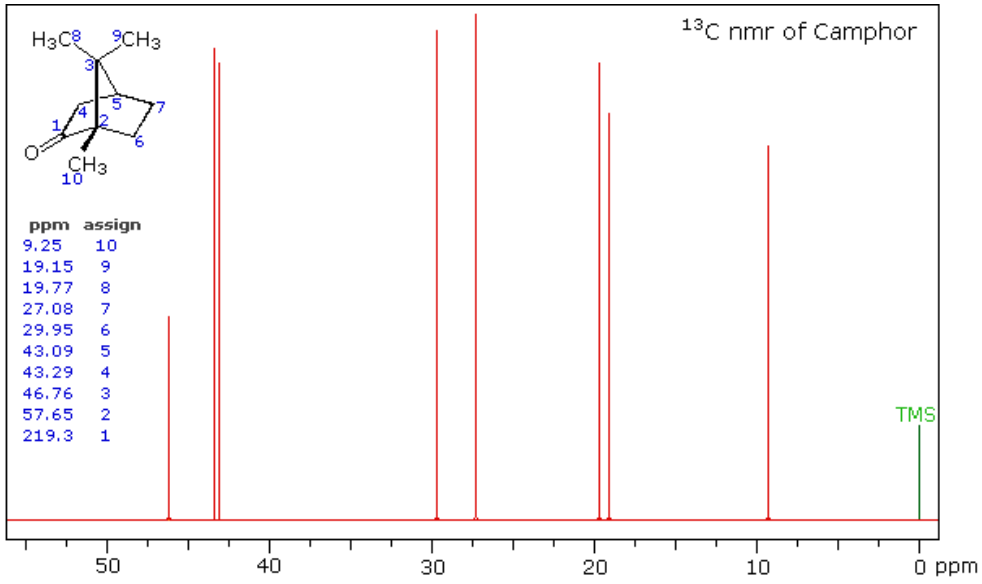


Additional Information from ^{13}C NMR Spectroscopy

Broad band decoupling of the hydrogen atoms in a molecule was an essential operation for obtaining simple (single line) carbon NMR spectra. The chemical shifts of the carbon signals provide useful information, but it would also be very helpful to know how many hydrogen atoms are bonded to each carbon. Aside from the fact that carbons having no bonded hydrogens generally give weak resonance signals, this information is not present in a completely decoupled spectrum.

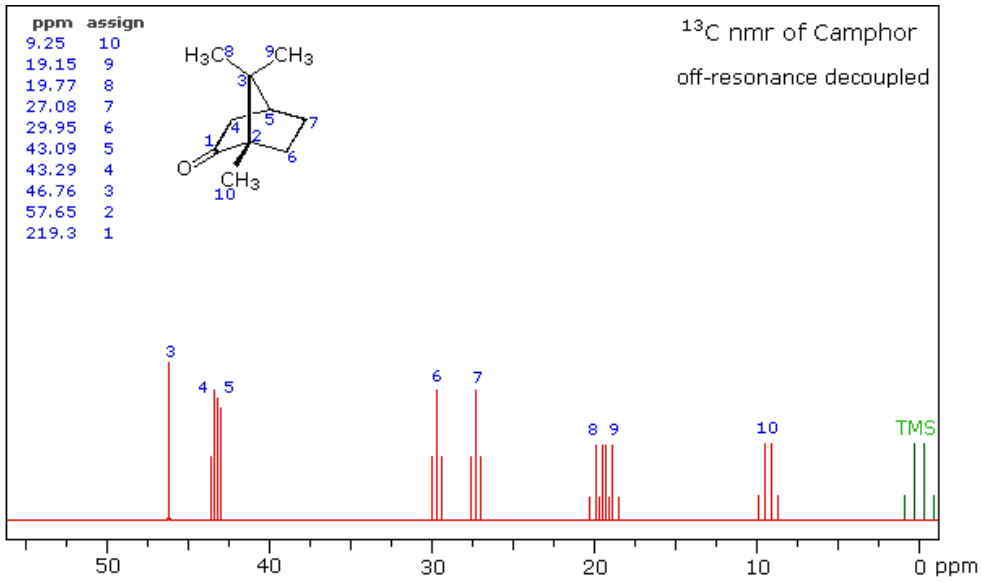


Clever methods of retaining the hydrogen information while still enjoying the benefits of proton decoupling have been devised. The techniques involved are beyond the scope of this discussion, but the overall results can still be appreciated. The ^{13}C NMR spectrum of camphor shown below will serve as an illustration. It will be helpful to view an expanded section of this spectrum from δ 0.0 to 50.0 ppm, and this will be presented in the High Field Expansion spectrum. The two lowest field signals are missing in the expanded display.



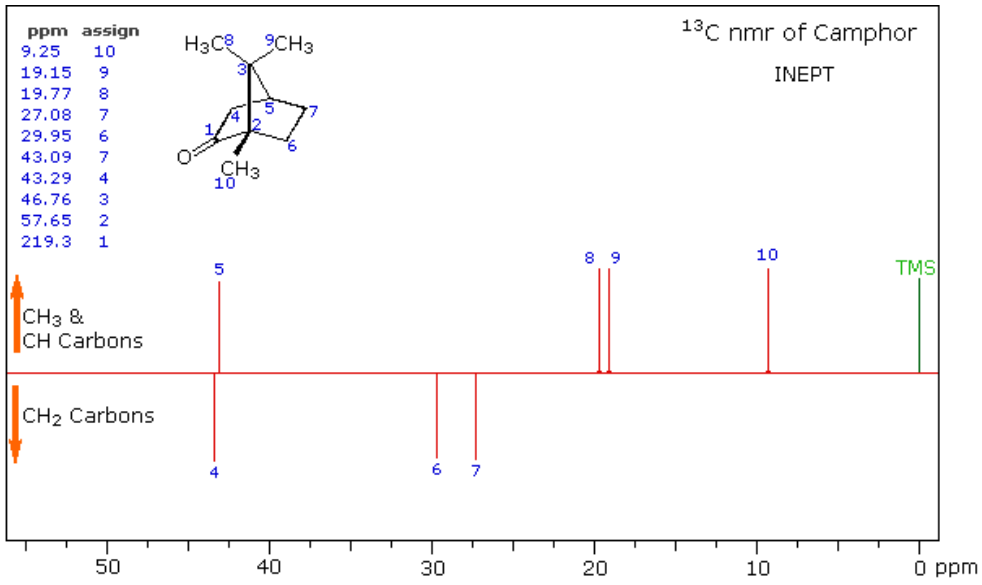
High Field Expansion of Camphor

Even though the expanded display now shows the distinct carbon signals clearly, the origin of each is ambiguous. An early method of regaining coupling information was by **off-resonance decoupling**. In this approach a weaker and more focused proton decoupling frequency is applied as the carbon spectrum is acquired. Vestiges of the C-H coupling remain in the carbon signals, but the apparent coupling constants are greatly reduced. View the Off-Resonance Decouple spectrum. The results of such an experiment will be displayed. Notice that all the methyl groups are quartets (three coupled hydrogens), the methylene groups are triplets and methine carbons are doublets. Overlap of two quartets near δ 19 ppm and the doublet and triplet near δ 43 ppm are complicating factors.



Off-Resonance Decouple Spectrum of Camphor

A better way for classifying the carbon signals is by a technique called **INEPT** (insensitive nuclear enhancement by polarization transfer). This method takes advantage of the influence of hydrogen on ^{13}C relaxation times, and can be applied in several modes. One of the most common applications of INEPT separates the signals of methyl and methine carbons from those of methylene carbons by their sign. Carbons having no hydrogen substituents have a zero signal.



INEPT Spectrum of Camphor

Properties of Some Deuterated NMR Solvents

Solvent	B.P. °C	Residual ^{1}H signal (δ)	Residual ^{13}C signal (δ)
acetone-d_6	55.5	2.05 ppm	206 & 29.8 ppm
acetonitrile-d_3	80.7	1.95 ppm	118 & 1.3 ppm
benzene-d_6	79.1	7.16 ppm	128 ppm

chloroform-d	60.9	7.27 ppm	77.2 ppm
cyclohexane-d_{12}	78.0	1.38 ppm	26.4 ppm
dichloromethane-d_2	40.0	5.32 ppm	53.8 ppm
dimethylsulfoxide-d_6	190	2.50 ppm	39.5 ppm
nitromethane-d_3	100	4.33 ppm	62.8 ppm
pyridine-d_5	114	7.19, 7.55 & 8.71 ppm	150, 135.5 & 123.5 ppm
tetrahydrofuran-d_8	65.0	1.73 & 3.58 ppm	67.4 & 25.2 ppm

Contributors

- William Reusch, Professor Emeritus (Michigan State U.), Virtual Textbook of Organic Chemistry
- Layne Morsch (University of Illinois Springfield)

This page titled 1.7: Supplemental NMR Topics is shared under a CC BY-NC-SA 4.0 license and was authored, remixed, and/or curated by William Reusch.

- Supplemental NMR Topics by William Reusch is licensed CC BY-NC-SA 4.0.

INDEX

R

resonance Raman spectroscopy
1.5: Raman Spectroscopy

S

SERS
1.5: Raman Spectroscopy

Stokes lines
1.5: Raman Spectroscopy

V

virtual state
1.5: Raman Spectroscopy

This page titled Molecular and Atomic Spectroscopy (Wenzel) is shared under a CC BY-NC 4.0 license and was authored, remixed, and/or curated by Thomas Wenzel via source content that was edited to the style and standards of the LibreTexts platform.

- Molecular and Atomic Spectroscopy (Wenzel) by Thomas Wenzel is licensed CC BY-NC 4.0. Original source: http://community.asdlib.org/activelearningmaterials/molecular-and-atomic-spectroscopy/.